Properties of a novel K^+ current that is active at resting potential in rabbit pulmonary artery smooth muscle cells

A. M. Evans, O. N. Osipenko and A. M. Gurney *

Department of Physiology and Pharmacology, University of Strathclyde, Royal College, 204 George Street, Glasgow G1 1XW, UK

1. An outward current ($I_{K(N)}$) was identified in rabbit pulmonary artery myocytes, which persisted after Ca^{2+}-activated and ATP-sensitive K^+ currents were blocked by TEA (10 mM) and glibenclamide (10 μM), respectively, and after A-like ($I_{K(A)}$) and delayed rectifier ($I_{K(V)}$) K^+ currents were inactivated by clamping the cell at 0 mV for >10 min. It was found in smooth muscle cells at all levels of the pulmonary arterial tree.

2. The relationship between the reversal potential of $I_{K(N)}$ and the extracellular K^+ concentration ($[K^+]_o$) was close to that expected for a K^+-selective channel. Deviation from Nernstian behaviour at low $[K^+]_o$ could be accounted for by the presence of an accompanying leakage current.

3. $I_{K(N)}$ is voltage gated. It has a low threshold for activation, between −80 and −65 mV, and activates slowly without delay. Activation follows an exponential time course with a time constant of 1·6 s at −60 mV. Deactivation is an order of magnitude faster than activation, with a time constant of 107 ms at −60 mV.

4. $I_{K(N)}$ showed a similar sensitivity to 4-aminopyridine as $I_{K(A)}$ and $I_{K(V)}$, with 49% inhibition at 10 mM. The current was not blocked by 10 μM quinine, which did inhibit $I_{K(A)}$ and $I_{K(V)}$, by 51 and 47%, respectively.

5. Activation of $I_{K(N)}$ was detected at potentials close to the resting membrane potential of pulmonary artery smooth muscle cells, under physiological conditions. Thus it is likely to contribute to the resting membrane potential of these cells.

The membrane potential and tone of vascular smooth muscle are strongly influenced by the activity of membrane K^+ channels (reviewed in Nelson & Quayle, 1995). A knowledge of the K^+ channel subtypes present within the smooth muscle cells of different arteries is, therefore, vital to our understanding of the physiological mechanisms that control cell and vessel function in different arterial beds. To date five different K^+ channel subtypes have been identified in arterial smooth muscle cells, namely those which underlie the nucleotide-regulated ($I_{K(ATP)}$; Quayle & Standen, 1994), Ca^{2+}-activated ($I_{K(Ca)}$; Benham, Bolton, Lang & Takewaki, 1986), delayed rectifier ($I_{K(V)}$; Beech & Bolton, 1989), A-like ($I_{K(A)}$; e.g. Clapp & Gurney, 1991) and inward rectifier ($I_{K(IR)}$; Edwards, Hirst & Silverberg, 1988) K^+ currents. Each of these K^+ currents can be distinguished on the basis of their pharmacology, Ca^{2+} sensitivity and/or voltage-dependent kinetics. With the exception of $I_{K(IR)}$, all of these currents have been identified in myocytes from rabbit pulmonary artery (Clapp & Gurney, 1991; Evans, Clapp & Gurney, 1994).

In isolated pulmonary arterial smooth muscle cells, $I_{K(ATP)}$ is identifiable as a time-independent, voltage-insensitive current, which is inhibited by intracellular ATP and extracellular sulphonylurea compounds like glibenclamide and activated by potassium channel openers such as levcromakalim (Clapp & Gurney, 1992). Activation of $I_{K(Ca)}$ is both voltage and time dependent, with activity increasing at positive membrane potentials and as the Ca^{2+} concentration at the cytoplasmic surface of the channel protein is increased (Clapp & Gurney, 1991; Robertson, Corry, Nye & Kozlowski, 1992). $I_{K(Ca)}$ can be separated from the other K^+ current subtypes present in pulmonary arterial myocytes, due to its selective block by tetraethylammonium ions (Clapp & Gurney, 1991; Robertson *et al.* 1992), or charybdotoxin (Yuan, 1995).

$I_{K(A)}$ and $I_{K(V)}$ are voltage-gated K^+ currents with little sensitivity to Ca^{2+}. They can be identified in pulmonary artery smooth muscle by their relative insensitivity to block by tetraethylammonium ions and glibenclamide (Clapp &

* To whom correspondence should be addressed.

Gurney, 1991; Evans *et al.* 1994; Smirnov, Robertson, Ward & Aaronson, 1994, Yuan, 1995) and by their sensitivity to block by 4-aminopyridine (Clapp & Gurney, 1991; Yuan, 1995). Although these two currents cannot, as yet, be separated from each other pharmacologically, they display distinct rates of activation and inactivation. $I_{K(A)}$ is a transient current that activates rapidly, peaks within the first 20 ms of a depolarizing voltage step, and inactivates completely within 100 ms (Clapp & Gurney, 1991). In contrast, $I_{K(V)}$ activates and inactivates more slowly, reaching peak activation within 100 ms of a depolarizing step (Evans *et al.* 1994; Smirnov *et al.* 1994; Yuan, 1995), while inactivation requires at least 60 s to reach steady state (Evans *et al.* 1994).

Of the K^+ current subtypes present, $I_{K(ATP)}$, $I_{K(Ca)}$ and $I_{K(V)}$ have all been implicated in the control of the resting potential and resting tone of pulmonary arteries (Clapp & Gurney, 1992; Post, Hume, Archer & Weir, 1992; Smirnov *et al.* 1994; Yuan, 1995). Thus studies of the roles of K^+ channels in the physiological and pathophysiological control of pulmonary arterial pressure have centred on the regulation of these three currents. In the present investigation we describe a novel voltage-gated K^+ current, which may play a significant role in the regulation of pulmonary arterial tone. This K^+ current has a threshold for activation between −80 and −65 mV, activates slowly without delay, is non-inactivating and has a distinct pharmacology.

METHODS

Cell isolation

Male New Zealand White rabbits (2–3 kg) were killed by intravenous injection of sodium pentobarbitone (80 mg kg^{-1}) and exsanguinated. The lungs with attached pulmonary artery were removed and placed in physiological salt solution (PSS) of the following composition (mM): NaCl, 124; KCl, 5; $NaHCO_3$, 15; $CaCl_2$, 1·8; $MgCl_2$, 1; NaH_2PO_4, 0·5; KH_2PO_4, 0·5; glucose, 10; Hepes, 15; Phenol Red, 0·04; adjusted to pH 7·3 by gassing with 95% O_2–5% CO_2. The lungs were separated into individual lobes and the intrapulmonary arteries dissected free of surrounding tissue with the aid of a dissection microscope. The main pulmonary arteries from outside and inside the lung, intrapulmonary arteries of diameter 200–400 μm and vessels < 200 μm were collected separately, diameters being measured with a calibrated reticle. Connective tissue was carefully removed from all arterial branches. The larger vessels were opened along the longitudinal axis and cut into 1 mm wide strips, while small vessels were cut into < 1 mm rings. Single smooth muscle cells were isolated from each preparation using a previously described method (Clapp & Gurney, 1991). Briefly, the muscle strips were washed in a low Ca^{2+} dissociation medium of the following composition (mM): NaCl, 110; KCl, 5; $NaHCO_3$, 15; $CaCl_2$, 0·16; $MgCl_2$, 2; NaH_2PO_4, 0·5; KH_2PO_4, 0·5; glucose, 10; Hepes, 15; Phenol Red, 0·04; EDTA, 0·49; taurine, 10; adjusted to pH 7·0 with 95% air–5% CO_2. They were then placed in dissociation medium containing 0·25 mg ml^{-1} papain (Fluka Chemicals Ltd, Dorset, UK) and 0·02% bovine serum albumin (fraction V, fatty acid and globulin free; Sigma) and stored overnight in a refrigerator. The following day 0·2 mM dithiothreitol (Sigma) was added to the enzyme solution containing the tissue and the solution warmed to 37 °C for 10 min. The tissue was then transferred to enzyme-free dissociation medium, and the smooth muscle cells isolated by trituration. Cells were stored in dissociation medium in a refrigerator until required.

Electrophysiology

Cells were transferred to a 400 μl experimental chamber, mounted on the stage of an inverted microscope, and superfused at ~0·5 ml min^{-1} with PSS at room temperature (22–25 °C). In some experiments cells were perfused with a high-K^+ PSS, which was prepared by replacing the NaCl in PSS with equimolar KCl and contained (mM): KCl, 129; $NaHCO_3$, 15; $CaCl_2$, 1·8; $MgCl_2$, 1; NaH_2PO_4, 0·5; KH_2PO_4, 0·5; glucose, 10; Hepes, 15; Phenol Red, 0·04. Low-Na^+ solution was prepared by replacing the NaCl with equimolar TEACl. All perfusing solutions were equilibrated with 95% O_2–5% CO_2 (pH 7·3).

K^+ currents were recorded under voltage clamp, using the whole-cell, patch-clamp technique with an Axopatch-1A or 200A patch-clamp amplifier (Axon Instruments Inc.). Patch pipettes (1–2 MΩ) were pulled from filamented borosilicate glass capillaries (Clark Electromedical Instruments, Pangbourne, UK) and filled with recording solution of the following composition (mM): KCl, 130; $MgCl_2$, 1; EGTA, 1; Hepes, 20; Na_2GTP, 0·5; pH adjusted to 7·2 with KOH. The junction potential between the pipette and bath solution (2–4 mV) was cancelled prior to pipette–cell contact. Reported voltages were not corrected for junction potential errors arising upon establishing the whole-cell configuration. The input resistance and cell capacitance were measured from the current response to a 10 mV hyperpolarizing step applied from −80 mV. Voltage commands were generated with pCLAMP data acquisition software (v. 5.5 and 5.7; Axon Instruments), through a Labmaster TM-40 (Scientific Solutions Inc., OH, USA) or Digidata 1200 (Axon Instruments) interface. Currents were filtered at 0·5–5 kHz, digitized at 1–16 kHz, and stored on disk using pCLAMP. During long recording periods, filtered records were additionally stored on DAT tape (DTR-1200 recorder; Biologic, Grenoble, France) or video tape (PCM-701ES digital audio processor and βmax recorder; Sony). Data analysis employed pCLAMP and ORIGIN (Microcal Software, Northampton, MA, USA) software. Current records are not leak subtracted unless stated. Data are quoted as means ± S.E.M, unless otherwise noted. Data were compared using Student's t test, unless otherwise indicated, and statistical significance was assumed if $P < 0·05$.

Chemicals

Stock solutions of TEACl (1 M; Fluka), $BaCl_2$ (1 M; Merck Ltd), charybdotoxin (10 μM; Peninsula Laboratories Europe Ltd, Merseyside, UK), iberiotoxin (10 μM; Sigma) and apamin (100 μM; Sigma) were prepared in 18 MΩ H_2O. Quinine sulphate (1 mM; Merck), 4-aminopyridine (4-AP, 10 mM; Sigma), digitoxin (Sigma), ouabain and clofilium tosylate (both from Research Biochemicals International, through Semat Technical (UK) Ltd, St Albans) were prepared daily in PSS, the pH of the 4-AP solution being adjusted to 7·3 before dilution. Glibenclamide (10 mM; Sigma) was dissolved in DMSO, which was present at 0·1% after dilution. At this concentration, DMSO by itself had no effect on the K^+ currents recorded. Fresh experimental solutions were prepared daily by dilution in PSS. Drugs were applied either to the PSS superfusing the bath or by microsuperfusion from a flow pipe (Langton, 1993).

RESULTS

Identification of a non-inactivating outward current with distinct pharmacology

Throughout the present investigation, $I_{K(ATP)}$ and $I_{K(Ca)}$ were blocked by the combined application of glibenclamide (10 μM) and TEA (10 mM) in the superfusate. From previous studies of pulmonary artery myocytes, the only K^+ currents thought to persist under these conditions are the 4-AP-sensitive $I_{K(A)}$ and $I_{K(V)}$ (Evans *et al.* 1994; Smirnov *et al.* 1994; Yuan, 1995). Both display voltage-dependent inactivation, which is maximal by −20 mV (Clapp & Gurney, 1991; Evans *et al.* 1994). However, even after prolonged periods (> 60 s) at −20 mV or more positive potentials there was a component of outward current that failed to inactivate (Okabe, Kitamura & Kuriyama, 1987; Evans *et al.* 1994). In the present study, the residual, non-inactivatable current amounted to 16 ± 2% ($n = 14$) of the total current activated by a test pulse to 40 or 60 mV from a holding potential of −80 mV. The experiments that follow were designed to elucidate the nature of this non-inactivating current.

Cells were clamped at 0 mV to maximally inactivate $I_{K(A)}$ and $I_{K(V)}$. The residual current, measured after 10 min at 0 mV, was 0·56 ± 0·05 pA pF^{-1} ($n = 15$). Subsequent application of a voltage ramp to −100 mV, immediately preceded by a step to 60 mV, revealed a non-linear dependence of the non-inactivating current on the membrane potential (Fig. 1). This was particularly evident between −40 and −100 mV, where the current displayed marked outward rectification, consistent with the deactivation of voltage-gated ion channels. In addition, slight inward rectification was often observed at potentials more positive than 40 mV. From the linear section of the current *versus* voltage relationship, we estimate the macroscopic conductance to be 2·5 ± 0·2 nS ($n = 8$).

Figure 2*A* demonstrates that 10 mM 4-AP, applied extracellularly by microsuperfusion, inhibited the non-inactivating current at 0 mV by 49 ± 8% ($n = 4$). At the same concentration, 4-AP inhibited $I_{K(A)}$ by 59 ± 8% and $I_{K(V)}$ by 56 ± 6% ($n = 6$; Fig. 2*B*). These latter currents were activated by a test pulse to 40 mV from a holding potential of −80 mV; $I_{K(A)}$ was measured as the peak current reached within 20 ms and $I_{K(V)}$ as the plateau current at 100 ms. In contrast, 10 μM quinine applied in the same way failed to inhibit the non-inactivating current measured at 0 mV (Fig. 2*C*), which remained at 98 ± 3% ($n = 10$) of the control. At the same concentration, quinine did, however, reduce the amplitudes of both $I_{K(A)}$ and $I_{K(V)}$ (Fig. 2*D*) by 51 ± 7% and 47 ± 9%, respectively ($n = 5$). This selective inhibition by quinine suggests that the non-inactivating current does not simply represent current carried by residual, non-inactivated $I_{K(A)}$ and/or $I_{K(V)}$, but that it is carried through distinct channels. Unfortunately, at higher concentrations, which were required for complete block of $I_{K(A)}$ and $I_{K(V)}$, quinine also reduced the non-inactivating current. This drug could not, therefore, be used to produce clear separation of the currents throughout their respective activation ranges. A number of other agents failed to block the non-inactivating current. These included TEA (124 mM, $n = 3$), which was applied by bath perfusion of PSS in which the TEA replaced Na^+ on an equimolar basis, charybdotoxin (300 nM, $n = 4$), iberiotoxin (250 nM, $n = 4$), $BaCl_2$ (1 mM, $n = 3$), ouabain (100 μM, $n = 5$), digitoxin (100 μM, $n = 5$), apamin (100 nM, $n = 3$) and clofilium (1 mM, $n = 3$), which were applied by microsuperfusion.

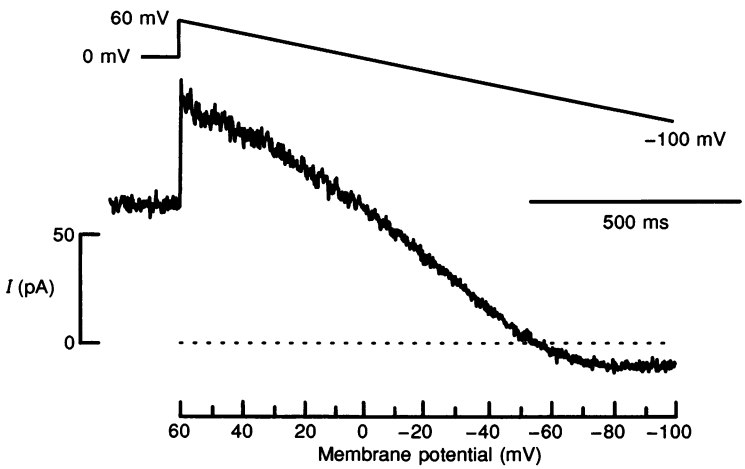

Figure 1. A non-inactivating outward current at 0 mV

Current *versus* voltage relationship of an outward current that failed to inactivate after voltage clamping the cell at 0 mV for 10 min. Trace shows current recorded during a 1·2 s voltage ramp to −100 mV immediately following a step to 60 mV, from a holding potential of 0 mV. Experiments carried out in the presence of extracellular TEA (10 mM) and glibenclamide (10 μM).

The non-inactivating outward current is a potassium current

As shown in Fig. 3*A*, increasing the extracellular potassium concentration ($[K^+]_o$) from 10 to 30 mM and then to 130 mM reduced the non-inactivating current recorded at 0 mV. It also caused a positive shift in the reversal potential of the current observed during a subsequent voltage ramp from 60 to −100 mV. With symmetrical transmembrane $[K^+]$ (130 mM), no outward current was seen at a holding potential of 0 mV and the current recorded during the voltage ramp reversed direction close to 0 mV. It is also noticeable that with symmetrical transmembrane $[K^+]$, the increased driving force for inward K^+ flux effectively amplified the current rectification observed in the negative region of the voltage ramp. The reversal potential, or the membrane potential at which there was no net flow of current, was measured from the current recorded during 1 s-long negative ramps from 60 to −100 mV, following a 5 min period at 0 mV. Figure 3*B* shows that the measured reversal potential varied in an essentially linear fashion with the logarithm of $[K^+]_o$. The Nernst equation for a perfectly K^+-selective conductance predicts a linear relation in such a plot, with slope of 58 mV decade^{-1}, as indicated by the continuous line in Fig. 3*B*. The experimental values lie close to the predicted line, although some deviation is apparent especially at low $[K^+]_o$. The measurements of reversal potential were made without leak subtraction, so it is likely that the current activated during the voltage ramp would be composed of a voltage-dependent current and a non-selective leak current. The finding that the current recorded during the voltage ramp reversed direction close to 0 mV in the presence of 130 mM K_o^+ is consistent with this idea, since both K^+-selective and leak currents would reverse at 0 mV under these conditions. Reducing the $[K^+]_o$ would be expected to shift the reversal potential of a K^+-selective current to more negative values, without affecting the leak current. Thus the reversal potential (E_0) of the combined current would be given by:

$$E_0 = \frac{g_K}{g_K + g_L} E_K + \frac{g_L}{g_K + g_L} E_L, \quad (1)$$

where E_K and E_L are the equilibrium potentials for the K^+

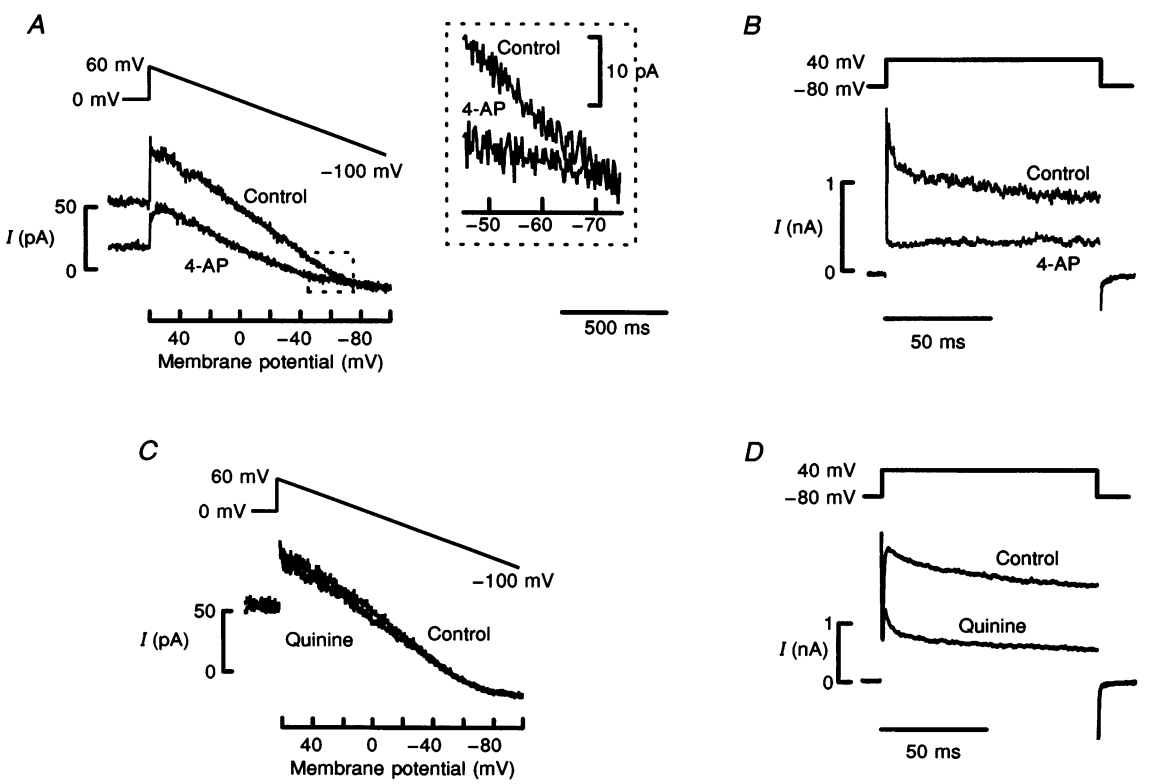

Figure 2. Pharmacological properties of the non-inactivating current differ from $I_{K(A)}$ and $I_{K(V)}$

A and *C*, current records obtained during a 1 s voltage ramp to −100 mV immediately following a step to 60 mV, applied from a holding potential of 0 mV, before and after application of 10 mM 4-AP (*A*) or 10 μM quinine (*C*). Each trace represents the mean of 3 individual records. The inset in *A* shows the area enclosed by the box on an expanded scale. *B* and *D*, records of $I_{K(A)}$ and $I_{K(V)}$ activated by a test pulse to 40 mV, from a holding potential of −80 mV, under control conditions and in the presence of 10 mM 4-AP (*B*) or 10 μM quinine (*D*).

(g_K) and leakage (g_L) conductances, respectively. Since $E_L = 0$ mV, eqn (1) can be simplified to:

$$E_0 = \frac{g_K}{g_K + g_L} E_K. \quad (2)$$

The dashed line in Fig. 3*B* shows that the observed relationship between E_0 and $[K^+]_o$ is well fitted by eqn (2), with $g_K/(g_K + g_L) = 0{\cdot}83$. Thus the deviation of the observed reversal potentials from the Nernst predictions for a K^+-selective conductance can be explained by assuming the presence of a parallel leak conductance, which contributes 17% of the total membrane conductance. Figure 3*C* shows that, in the presence of 5 mM K_o^+, removing the extracellular NaCl and replacing it with TEACl (124 mM) had little effect on the current recorded during a voltage ramp from 60 mV to −100 mV and the reversal potential was unchanged. Thus it is unlikely that Na^+ ions contribute to the non-inactivating current. The current was, however, abolished when the K^+ in the pipette solution was replaced with Cs^+ ($n = 4$), providing further evidence that K^+ is the main permeant ion. Since the non-inactivating current is most likely to be carried through K^+-selective channels, we accordingly denote it $I_{K(N)}$.

Deactivation of $I_{K(N)}$

After clamping myocytes at 0 mV for 10 min to isolate $I_{K(N)}$ from $I_{K(A)}$ and $I_{K(V)}$, negative voltage steps in the range −40 to −110 mV induced current relaxations consistent with the deactivation of voltage-gated channels. Current relaxations were measured in high (130 mM) $[K^+]_o$, to amplify the currents at negative potentials, where K^+ currents were inward. Figure 4*A* shows current relaxations evoked during 100 ms test pulses to −40, −60 and −100 mV applied from a holding potential of 0 mV. An increasing proportion of the current deactivated as the test pulse became more negative (Fig. 4*A*). As illustrated in Fig. 4*B*, there was a sigmoidal relationship between the proportion of the current that deactivated and the amplitude of the test potential, with deactivation minimal above −40 mV and maximal below −80 mV. The membrane potential at which half-maximal deactivation occurred ($V_{½}$) was estimated by fitting the data in Fig. 4*B* with a Boltzmann function of the form:

$$I = \frac{I_{max}}{1 + \exp[(V_{½} - V)/k]}, \quad (3)$$

where I is the proportion of the total current that deactivated at a given membrane potential, I_{max} is the maximum

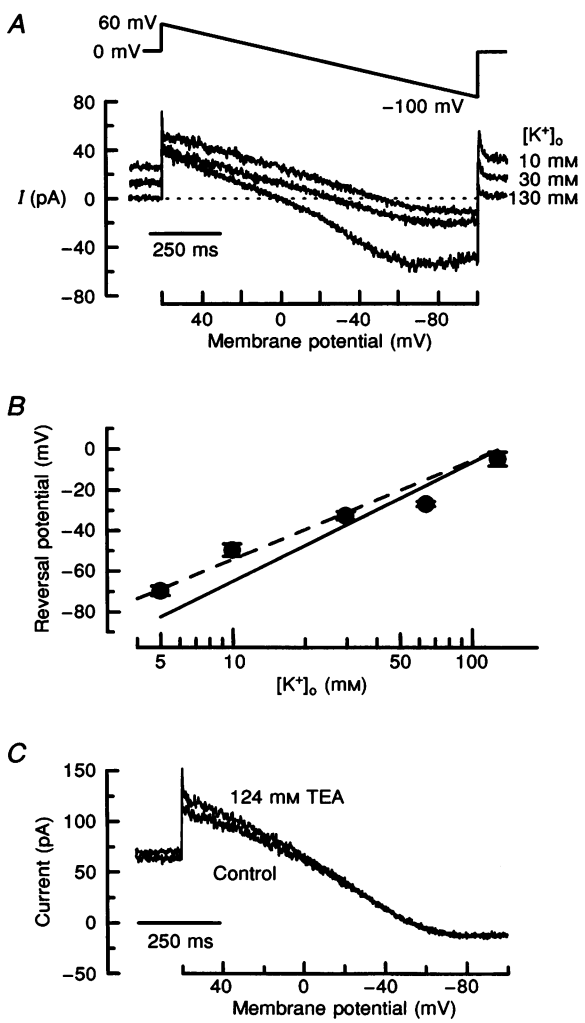

Figure 3. The non-inactivating outward current is carried by a K^+-selective conductance

A, currents recorded during a 1 s voltage ramp to −100 mV, immediately following a step to 60 mV, applied after holding the cell at 0 mV for 10 min to inactivate $I_{K(A)}$ and $I_{K(V)}$. Records shown were obtained from the same cell, in the presence of 10, 30 and 130 mM K_o^+, prepared by equimolar substitution of K^+ for Na^+ in the superfusate. Raising $[K^+]_o$ reduced the outward current measured at 0 mV and shifted the reversal potential to more positive values. *B*, plot of the reversal potential as a function of $[K^+]_o$ on a logarithmic scale. Points and vertical bars represent the means and S.E.M. of 3–8 observations, not corrected for junction potential errors. The continuous line represents the relationship predicted by the Nernst equation for a perfectly K^+-selective current, with a slope of 58 mV decade^{-1}. The dashed line represents the best fit of eqn (2) to the data, with $g_K/(g_K + g_L) = 0{\cdot}83$. *C*, records obtained as in *A*, in the presence of 5 mM external K^+, under control conditions and after equimolar replacement of the NaCl in the bathing solution with TEACl.

proportion that could be deactivated, V is the test potential and k a factor describing the steepness of the voltage dependence. The best fit, shown as the continuous curve in Fig. 4*B*, gave values for $V_{½}$ and k of −53 and 13 mV, respectively.

The time course of the deactivating current was well fitted by a single exponential (Fig. 4*A*), with time constant (τ_d) of 43 ± 8 ms ($n = 4$) at −100 mV and 107 ± 4 ms ($n = 3$) at −60 mV. The time constant displayed a fairly shallow dependence on membrane potential, increasing e-fold with 49 mV depolarization (Fig. 4*C*). The estimates of τ_d and its voltage dependence predict that current deactivation would reach steady-state at each potential during a hyperpolarizing ramp from 0 mV, provided the voltage was changed at a rate > 200 ms mV^{-1}. The steady-state current *versus* voltage relationship obtained using such a protocol is illustrated in Fig. 4*D*. In these experiments, the voltage was stepped to −40 mV immediately before ramping to more negative potentials. This step should have minimized contamination of the measured current by recovered $I_{K(A)}$ and $I_{K(V)}$, since −40 mV is close to the threshold for activation of these currents (see below). Thus the protocol should resolve the steady-state current *versus* voltage relationship for $I_{K(N)}$. From such steady-state records ($n = 9$), deactivation could first be detected at −47 ± 1 mV and appeared to be maximal by −78 ± 3 mV. This range agrees fairly well with the voltage range for deactivation estimated from the currents evoked by hyperpolarizing steps. Together these findings suggest that the threshold for activation of $I_{K(N)}$ lies positive to −80 mV, it is half-activated at −53 mV and fully activated above −40 mV.

Current activation during brief voltage steps

Since the previous results suggest that $I_{K(N)}$ has a low voltage threshold for activation, we looked for activation at

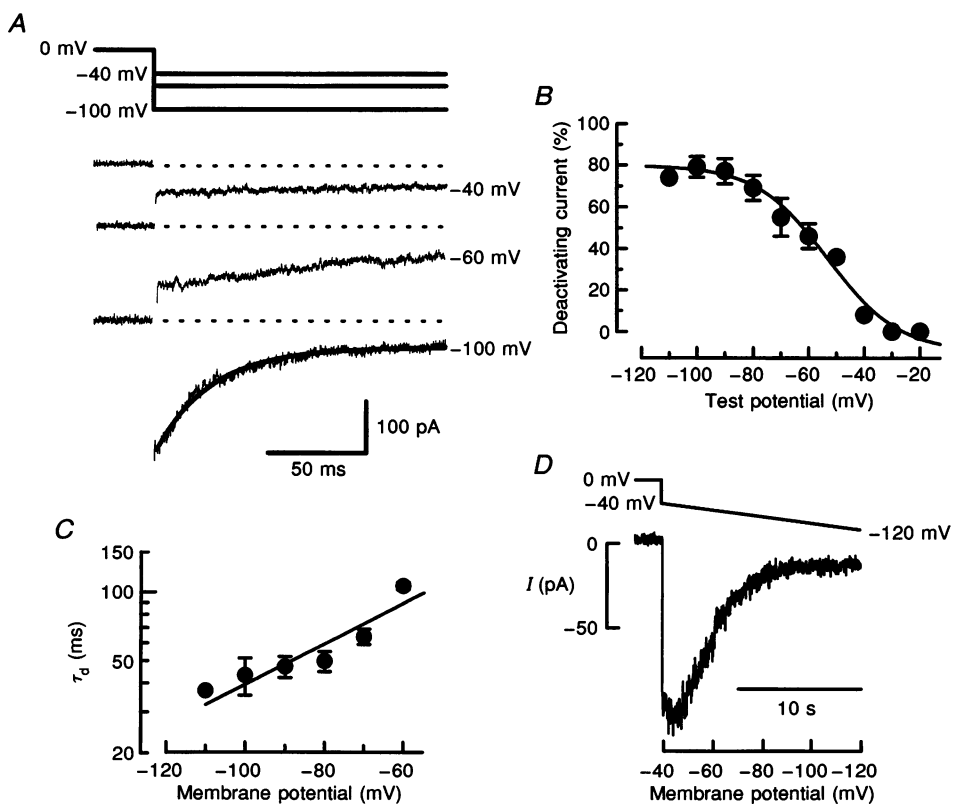

Figure 4. Voltage dependence of current deactivation

Currents were recorded with 130 mM K_o^+, resulting in inward K^+ currents at negative potentials. Voltage protocols were applied from a holding potential of 0 mV, after inactivation of $I_{K(A)}$ and $I_{K(V)}$. *A*, currents evoked by 100 ms steps to −40, −60 and −100 mV. The records are displaced vertically for clarity, with zero current indicated for each record by a dashed line. Inward current relaxations were pronounced at −100 mV, but not at −40 mV. The curve superimposed on the relaxation at −100 mV is the best fit exponential, with a time constant of 32 ms. *B*, relationship between the amplitude of the deactivating current and the test potential. The curve shows the best fit to eqn (3), with $V_{½} = -53$ mV and $k = 13$ mV. *C*, relationship between the time constant for current deactivation and membrane potential. The fitted line represents an e-fold change in the time constant for 49 mV depolarization (τ_d). Points and bars represent the means ± S.E.M. of at least 3 observations in *B* and *C*. *D*, current recorded during an 18 s voltage ramp from −40 to −120 mV. Deactivation began around −45 mV and was maximal by −81 mV. Approximately 55% deactivation is apparent at −60 mV.

negative potentials by applying 100 ms depolarizing steps from a holding potential of −80 mV. Figure 5*A* shows the maximum amplitude of the current plotted as a function of the test potential, in the presence of physiological (5 mM) and high (130 mM) $[K^+]_o$. In physiological $[K^+]_o$, the threshold for current activation was around −40 mV, with current rarely observed at more negative potentials (Fig. 5*B*). When $[K^+]_o$ was raised to 130 mM, a current that appeared to reach a plateau in around 100 ms was detected at −50 mV (Fig. 5*C*). But even under these conditions no voltage-gated current could be resolved at more negative potentials. Increasing the $[K^+]_o$ had only a small effect on the time course of current activation. In most cells the activation of $I_{K(A)}$ and $I_{K(V)}$ overlapped, resulting in the appearance at positive potentials of transient ($I_{K(A)}$) and sustained ($I_{K(V)}$) components, which followed a similar time course in low (Fig. 2*B* and *D*) and high (Fig. 5*C*) $[K^+]_o$. This precluded separate measurements of the rate constants for activation of $I_{K(A)}$ and $I_{K(V)}$. Instead we measured the time taken for the mixed current to reach a maximum level. This is compared in low and high $[K^+]_o$ over a range of potentials in Fig. 5*D*. Raising the $[K^+]_o$ from 5 to 130 mM appeared to slow the time to peak current at negative potentials. The effect was, however, small, and significant only at −40 mV, where the current took 63 ± 3 ms ($n = 17$) to reach maximum in low $[K^+]_o$ compared with 86 ± 4 ms ($n = 4$) in high $[K^+]_o$. The simplest explanation for these results is that extracellular K^+ lowers the threshold for activation and slows the gating kinetics of $I_{K(V)}$ and/or $I_{K(A)}$. Such effects have been demonstrated previously for neuronal delayed rectifier channels (e.g. Swenson & Armstrong, 1981; Safronov & Vogel, 1995). Despite the evidence in Fig. 4 that a substantial proportion of $I_{K(N)}$ is active at −60 mV, we were unable to resolve activation of a current below −50 mV during 100 ms steps, even in high $[K^+]_o$.

The non-inactivating K^+ current activates slowly

Figure 6*A* illustrates the compound K^+ current activated during a slow (15 s) voltage ramp from −140 to 40 mV, applied from a holding potential of −80 mV. High (130 mM) $[K^+]_o$ was employed to amplify current at negative potentials. Inward current was first seen to activate at −65 ± 2 mV ($n = 8$). The compound current was sensitive to block by both 4-AP and quinine, applied by microsuperfusion, although in both cases the degree of inhibition varied with the membrane potential. At 10 mM, 4-AP caused

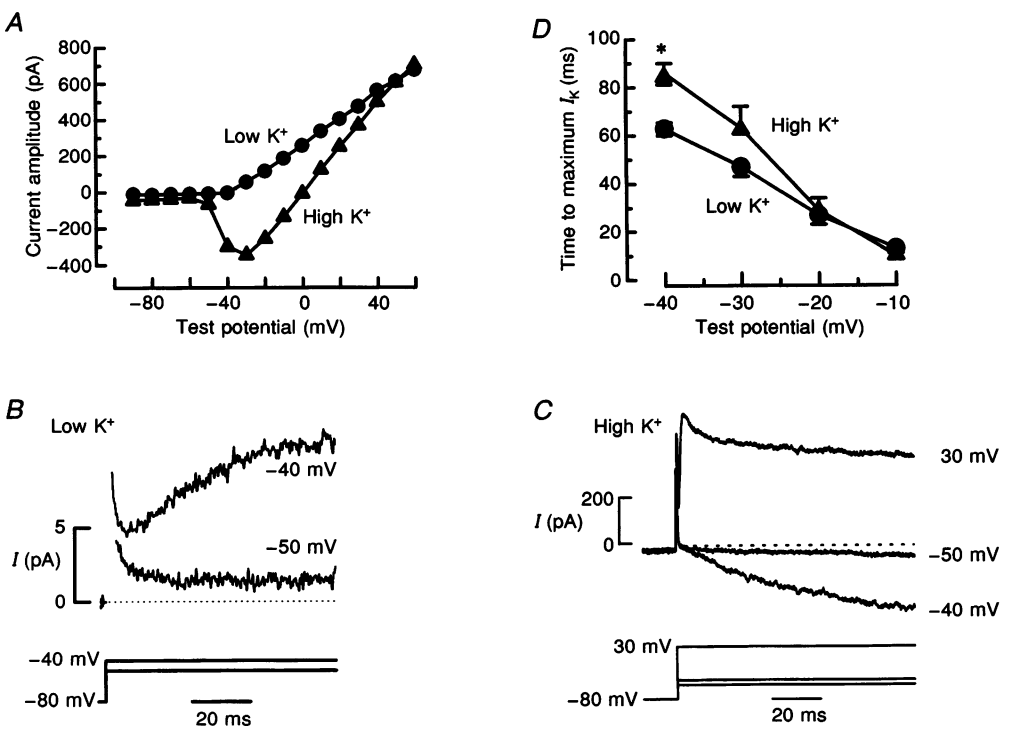

Figure 5. Current activated during brief voltage steps

Currents were activated by depolarizing steps applied from a holding potential of −80 mV. *A*, maximum amplitude of currents activated during 100 ms steps, plotted as a function of the test potential in the presence of 5 mM (low; ●) or 130 mM (high; ▲) K_o^+. *B*, currents activated by steps to −50 and −40 mV in the presence of 5 mM K_o^+. Traces show the mean currents generated by averaging individual records from 9 different cells. *C*, currents activated by steps to −50, −40 and 30 mV in the presence of 130 mM K_o^+. *D*, the time taken for the current to reach its maximum amplitude plotted as a function of the test potential, when steps were applied in the presence of 5 mM (●) or 130 mM (▲) K_o^+. Symbols and bars represent the means ± S.E.M. of 17 (5 mM K^+) and 4 (130 mM K^+) observations. * $P < 0{\cdot}05$ in comparing high with low $[K^+]_o$.

pronounced inhibition of the current at all membrane potentials. However, in the presence of 1 mM 4-AP, two clear 'humps' of activated current were revealed (Fig. 6*A*). The first 'hump' had an apparent threshold at −65 mV, more negative than expected for $I_{K(V)}$ and $I_{K(A)}$, whereas the second 'hump' appeared to activate in the appropriate voltage range for these two current types. Application of 10 μM quinine, which inhibited $I_{K(V)}$ and $I_{K(A)}$, but not $I_{K(N)}$ (Fig. 2), had little effect on the compound current activated between −65 and −50 mV, while it strongly suppressed the current at more positive potentials (Fig. 6*B*). These results are consistent with the existence of a low-threshold, voltage-gated current that is distinct from $I_{K(V)}$ and $I_{K(A)}$.

The appearance of current at negative potentials during slow voltage ramps, but not during brief steps, suggests that the low-threshold current might activate slowly. We therefore looked again for a voltage-gated current with low activation threshold by applying long (20 s) voltage steps to potentials between −80 and −50 mV, from a holding potential of −100 mV. During such long pulses, current could be clearly seen to activate at −60 mV, and often at more negative potentials. Figure 6*C* shows currents recorded during voltage

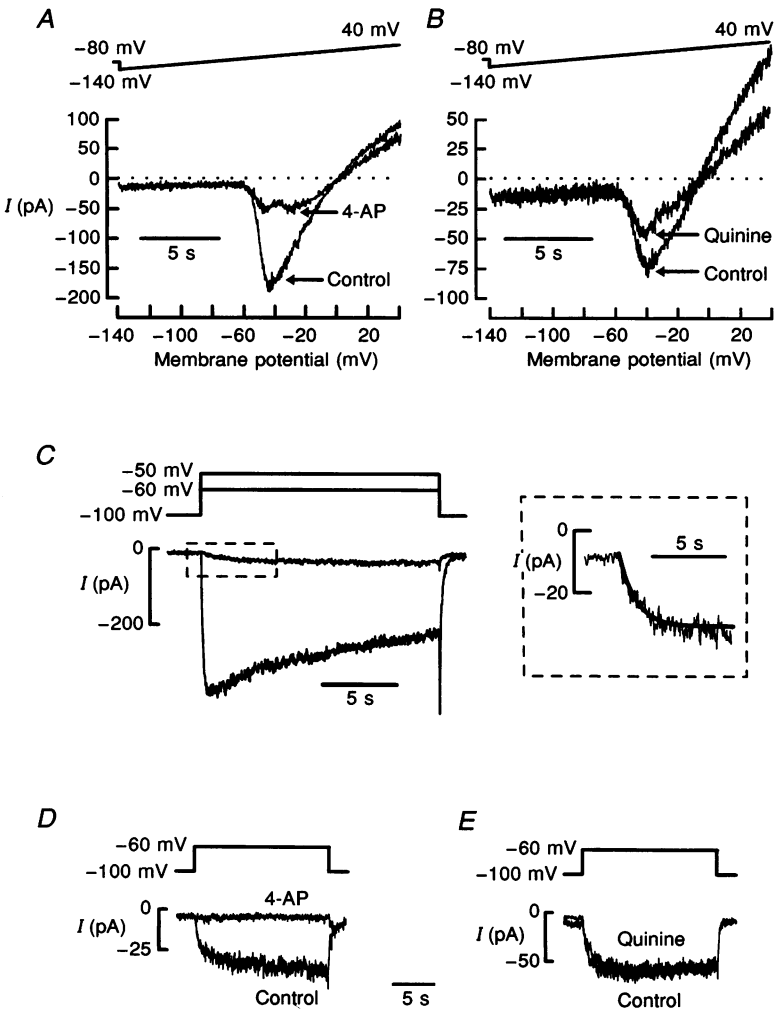

Figure 6. Evidence for a low-threshold slowly activating, non-inactivating K^+ current

Currents were recorded in 130 mM K^+_o. *A*, compound current activated during a 15 s voltage ramp from −140 to 40 mV, applied from a holding potential of −80 mV, in the absence (Control) and presence of 1 mM 4-AP. The threshold for current activation was −67 mV before and after 4-AP application. *B*, compound current recorded with the same protocol, in the absence (Control) and presence of 10 μM quinine. *C* (left-hand panel), currents activated by 20 s test pulses to −60 mV and −50 mV from a holding potential of −100 mV. A slowly activating, non-inactivating current is apparent at −60 mV, with an additional more rapidly activating, inactivating component recruited at −50 mV. The right-hand panel shows, on expanded scales, the section of the −60 mV current highlighted by the box. The curve superimposed on the current trace is the best fit exponential, with a time constant of 1·5 s. *D*, current evoked by a test pulse to −60 mV, under control conditions and following the application of 10 mM 4-AP. *E*, current evoked by a test pulse to −60 mV under control conditions and following the application of 10 μM quinine.

steps to −60 and −50 mV. At −60 mV, a slowly activating, non-inactivating current with an amplitude of 23 ± 5 pA ($n = 10$) was evoked. It activated without delay (Fig. 6*C*, right-hand panel), along a time course that was well fitted by a single exponential with time constant (τ_a) of 1·6 ± 0·4 s ($n = 4$). With such a slow time constant, only 6% of the current would be activated in 100 ms, so it would simply have been too small at 100 ms to be resolved during short voltage steps. At −50 mV a more rapidly activating, inactivating current was also evoked. This presumably represents $I_{K(V)}$ and/or $I_{K(A)}$, seen to activate during brief steps to −50 mV in high $[K^+]_o$. The pharmacology of the slowly activating current resembled that of $I_{K(N)}$ recorded at 0 mV in the presence of a physiological transmembrane $[K^+]$ gradient. Figure 6*D* shows that when evoked by a test pulse from −100 mV to −60 mV, the slowly activating current was abolished by microsuperfusion of 10 mM 4-AP ($n = 4$). In contrast, as shown in Fig. 6*E*, 10 μM quinine failed to inhibit this current. In fact, it caused augmentation in five out of ten cells, the current increasing on average by 53 ± 15% relative to control ($n = 10$). The rapidly activating, inactivating component of current recruited at −50 mV was inhibited both by 10 mM 4-AP and 10 μM quinine (not shown). This supports the hypothesis that the low-threshold, non-inactivating current is carried through channels that are distinct from those carrying $I_{K(A)}$ and $I_{K(V)}$.

Evidence for a low-threshold, slowly activating current in physiological $[K^+]_o$

Although the results presented in Fig. 4 predict that $I_{K(N)}$ would be more than 50% activated at −50 mV, its amplitude would be small in physiological conditions due to the low driving force for K^+ efflux. Nevertheless, an outward current could be detected at negative membrane potentials in the presence of physiological $[K^+]_o$. This is clear in the inset of Fig. 2*A*, which demonstrates the presence of a 4-AP-sensitive current at potentials negative to −60 mV, when examined after inactivation of $I_{K(A)}$ and $I_{K(V)}$ at 0 mV. Even in the absence of 4-AP, a net outward current could be detected at −50 mV (Fig. 1), provided the input resistance was high and linear leak current was small. In twelve cells with an input resistance >10 GΩ (mean: 18 ± 3 GΩ), the mean outward current measured at −50 mV in 5 mM K_o^+ was 7 ± 6 pA, equivalent to a conductance of 5 ± 5 pS pF^{-1}. As shown in Fig. 7*A*, it was also possible to detect a small, slowly activating outward current during long voltage steps to −50 mV, applied from a holding potential of −80 mV. Due to the low signal-to-

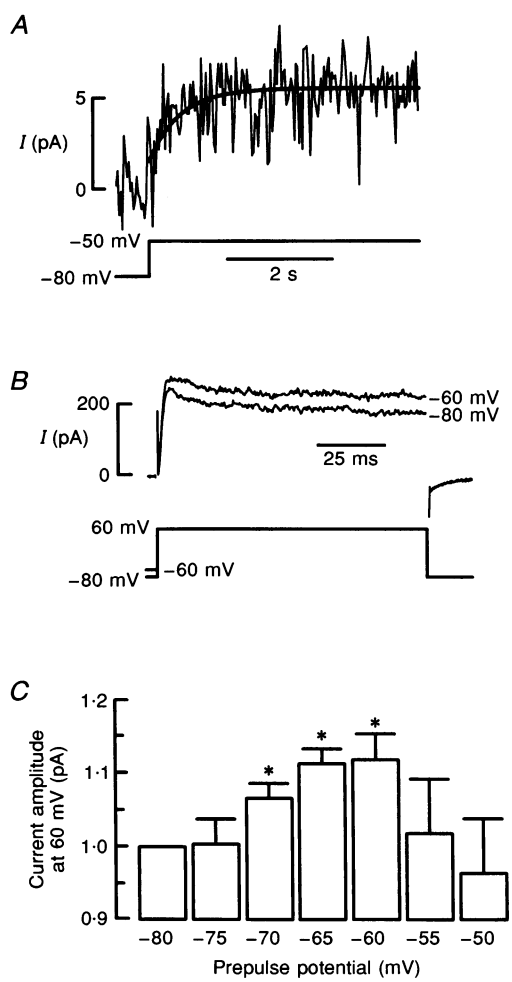

Figure 7. Evidence for a low-threshold current under physiological conditions

A, activation of an outward current at −50 mV in the presence of 5 mM K_o^+. The trace shows the mean record generated by leak subtracting and averaging individual records collected from 9 different cells, in response to a 5 s step from −80 mV to −50 mV. *B*, outward current evoked by a 100 ms step to 60 mV, applied from a holding potential of −80 mV, with or without a 60 s prepulse to −60 mV. *C*, histogram showing the effect of the prepulse potential on the amplitude of the current recorded in response to a 100 ms test pulse to 60 mV. One-way analysis of variance (ANOVA) with repeated measures gave $F = 2·6$ and $P < 0·05$ for all data between −80 and −60 mV. *$P < 0·05$ for individual comparisons with −80 mV.

noise ratio, it was not always possible to distinguish this component convincingly in individual current records, but it was resolvable when several records were averaged. The record in Fig. 7*A* was generated by leak subtracting and averaging the currents evoked in nine separate cells. The mean amplitude of the current between 4 and 10 s after the step was 5·6 pA, equivalent to a conductance of 112 pS. The time course of activation was fitted by an exponential with a time constant of 0·6 s. This compares fairly well with the rate of activation of the low-threshold current observed in high $[K^+]_o$ (Fig. 6*C*), but is an order of magnitude slower than the activation of $I_{K(A)}$ and $I_{K(V)}$ recorded at −40 mV from the same cells (Fig. 5*B*). This is consistent with the presence of a low-threshold current distinct from $I_{K(A)}$ and $I_{K(V)}$, which activates slowly under physiological conditions.

Comparison of the amplitudes of outward currents evoked from different holding potentials provides further evidence for a low-threshold K^+ current in physiological $[K^+]_o$. Figure 7*B* shows that the amplitude of the outward current evoked by a 100 ms step to 60 mV from a holding potential of −80 mV appeared larger if the step was preceded by a 60 s prepulse to −60 mV. The magnitude of the 'recruited' current varied with the prepulse potential as shown in Fig. 7*C*. A prepulse to −75 mV had little effect, but the current evoked at 60 mV gradually increased in amplitude as the prepulse became more positive, with the maximal effect being reached by −60 mV. Thereafter, the amplitude of the current declined, due to voltage-dependent inactivation of $I_{K(A)}$ and $I_{K(V)}$. This finding can be explained by the recruitment of an additional low-threshold, voltage-gated current during the prepulse. Moreover, the voltage range over which recruitment occurred is similar to the voltage range over which the low-threshold, voltage-gated $I_{K(N)}$ was found to activate in high $[K^+]_o$.

Distribution of the low-threshold current in the pulmonary arterial tree

A low-threshold, slowly activating current with the properties of $I_{K(N)}$ was recorded from smooth muscle cells isolated from the main pulmonary artery ($n = 20$), the main intrapulmonary artery ($n = 4$) and from branches of the intrapulmonary artery of 200–400 μm external diameter ($n = 6$). The current record shown in Fig. 6*D* was recorded from a smooth muscle cell isolated from a resistance-sized intrapulmonary artery of < 200 μm external diameter.

DISCUSSION

This study describes a K^+-selective current, $I_{K(N)}$, that was found in smooth muscle cells isolated from all branches of the rabbit pulmonary arterial tree, from the large artery entering the lung to the small, resistance-sized intrapulmonary vessels. Certain properties of the current distinguish it from previously described K^+ currents. It is voltage gated with a low threshold for activation, it activates slowly without delay, does not inactivate during prolonged depolarization and has a distinct pharmacology. The voltage dependence of $I_{K(N)}$ predicts that it would be active at the resting membrane potential (E_m), which lies between −55 and −60 mV in the intact tissue (Casteels Kitamura, Kuriyama & Suzuki, 1977*a*; Haeusler & Thorens, 1980) and around −55 mV in isolated myocytes (Clapp & Gurney, 1991, 1992). The main ions thought to contribute to the resting potential are K^+ and Cl^- (Casteels *et al.* 1977*a*). However, since the Cl^- conductance in pulmonary artery smooth muscle cells is Ca^{2+} dependent (Sutter, Turner, Albarwani, Clapp & Kozlowski, 1995), its contribution would be minimal under resting conditions and under the conditions of our experiments. The resting potential is therefore determined by a K^+ conductance in parallel with a leakage conductance. Since it is the potential at which the net membrane current is zero, it is defined in the same way as the reversal potential, according to eqns (1) and (2), where $E_m = E_0$.

In our experiments at 5 mM K_o^+, E_K was −82 mV. There is no evidence for the existence in these cells of ion-selective channels that open at potentials more negative than −80 mV, apart from K_{ATP} channels, which were blocked in the present study with glibenclamide (Clapp & Gurney, 1991, 1992). Thus the membrane resistance measured at these potentials should reflect only the leakage conductance. The resistance of 18 GΩ (see also Clapp & Gurney, 1991, 1992), measured between −80 and −90 mV, gives a value for g_L of 56 pS. Substituting these values for E_K and g_L into eqn (2) predicts that a K^+ conductance of 114 pS would be required to maintain the resting potential at its normal level of −55 mV. The actual contribution of voltage-gated K^+ conductances can be measured from the amplitude of the outward current activated by voltage steps to the resting potential, from a negative holding potential. The amplitude of the current shown in Fig. 7*A*, evoked by stepping from −80 to −50 mV in physiological $[K^+]_o$, is independent of the leak current and therefore provides our best estimate of the K^+ conductance active around the resting potential. The current was very small, so measurement of its amplitude was subject to error. Nevertheless, it provided a value for the conductance of 112 pS, which is remarkably close to the value predicted from eqn (2). Furthermore, the current evoked during this voltage step primarily reflected $I_{K(N)}$, because it activated below the threshold of, and an order of magnitude more slowly than $I_{K(A)}$ and $I_{K(V)}$. This suggests that $I_{K(N)}$ may make an important contribution to the resting potential of rabbit pulmonary artery myocytes, which would be determined by a balance between the outward current through $I_{K(N)}$ and any opposing inward current. This is consistent with recent reports showing that 4-AP-sensitive K^+ channels are the major contributors to the resting potential in pulmonary artery smooth muscle cells (Post, Gelband & Hume, 1995; Yuan, 1995). Moreover, since activation of $I_{K(N)}$ appears to be about 50% at the

resting potential, stability could be maintained by the opening or closing of $I_{K(N)}$ channels in response to depolarizing or hyperpolarizing influences. The properties of $I_{K(N)}$ are therefore well suited to a role in membrane potential regulation

Contributions of different K^+ channels to the resting membrane potential

Different K^+ channels contribute to the resting potential in other types of vascular smooth muscle. Inward rectifier (K_{IR}) channels are likely to be important in small arteries and arterioles, where they contribute around 1 pA of outward current (Nelson & Quayle, 1995). A preliminary report (Turner, Chang, Brown & Kozlowski, 1996) suggests that K_{IR} channels may be present in rat pulmonary artery smooth muscle. Their contribution to the resting potential of these cells will, however, be small, because pulmonary artery smooth muscle depolarizes and contracts when the $[K^+]_o$ is raised from 5 to 15 mM (Casteels Kitamura, Kuriyama & Suzuki, 1977*b*; Suzuki & Twarog, 1982). Hyperpolarization and relaxation would be expected if K_{IR} channels were major contributors to the resting potential (Nelson & Quayle, 1995). $I_{K(Ca)}$ has been identified in virtually every smooth muscle, so is likely to play an important physiological role. Spontaneous transient outward currents (STOCS) carried through K_{Ca} channels have been proposed to maintain membrane hyperpolarization and vasodilatation in pressurized, myogenic arteries (Brayden & Nelson, 1992; Nelson *et al.* 1995). At negative potentials, STOCS represent the simultaneous opening of two to thirteen K_{Ca} channels (Trieschmann & Isenberg, 1989; Nelson *et al.* 1995). For a single channel current of 0·5 pA at −55 mV (Benham *et al.* 1986), this would generate a whole-cell current of up to 6·5 pA, comparable to the outward current carried by $I_{K(N)}$ in the present study. However, pulmonary artery smooth muscle cells rarely display STOCS, and only at positive potentials (Clapp & Gurney, 1991; Lee & Earm, 1994). In addition, blockers of $I_{K(Ca)}$ have no effect on the resting potential of these cells (Post *et al.* 1995; Yuan, 1995). Furthermore, due to low vascular tone, pulmonary arterial pressure is normally less than 20% of that in the systemic circulation. Although blockers of $I_{K(Ca)}$ depolarized and contracted pressurized arteries, their effects were negligible when intravascular pressure was reduced to 15 mmHg (Brayden & Nelson, 1992; Nelson & Quayle, 1995), the average pressure in the pulmonary circulation. This suggests that the main role of K_{Ca} channels in pulmonary arteries is not to control membrane potential at rest, but to respond to stimulus-induced elevations in the cytosolic $[Ca^{2+}]$, thereby promoting repolarization to limit Ca^{2+} influx and contraction. In some blood vessels, K_{ATP} channels may contribute to the resting potential (Quayle & Standen, 1994). In pulmonary arteries, where glibenclamide has little effect on the resting potential or resting tone (Clapp & Gurney, 1992; Yuan, 1995), they are more likely to function as sensors of cellular metabolism, or as targets for endogenous vasodilators (Quayle & Standen, 1994). Of the K^+ currents known to exist in pulmonary artery smooth muscle, $I_{K(N)}$ may, therefore, make the major contribution to the resting potential and resting tone. However, since $I_{K(N)}$ deactivates as the membrane potential shifts towards E_K, its contribution to the resting potential would diminish towards zero if K_{Ca} or K_{ATP} channels were opened to induce hyperpolarization.

The potassium selectivity of $I_{K(N)}$

The K^+ selectivity of $I_{K(N)}$ is suggested by the closeness of the relationship between the reversal potential of the non-inactivating current and $[K^+]_o$ to that predicted by the Nernst equation for a perfectly K^+-selective ion channel. Although there was some deviation between the measured reversal potentials and the predicted values at low $[K^+]_o$, this could largely be accounted for by the presence of a parallel leak current, which was not subtracted before the reversal potentials were measured. Partial deactivation of $I_{K(N)}$ during the 1 s-long negative voltage ramp might be expected to reduce its contribution to the total current, thereby shifting the apparent reversal potentials to more positive values. This effect would have its greatest influence at 5 mM K^+, when the reversal potential was around −70 mV. Its contribution would, however, be small at higher $[K^+]_o$, when the reversal potentials were all above −50 mV, since little deactivation of $I_{K(N)}$ was observed during negative voltage steps to these potentials. Other factors that can influence the apparent relationship between the reversal potential of a K^+ current and the $[K^+]_o$ include: (1) the junction potential expected to occur when establishing the whole-cell configuration; (2) limited Na^+ permeation of the ion channels underlying $I_{K(N)}$, which has been shown to occur with delayed rectifier channels in K^+-free conditions (Callahan & Korn, 1994); and (3) accumulation of K^+ around the extracellular mouth of the channel while holding the cell at 0 mV. The junction potential error in this study was small (−2 to −4 mV) and would have shifted the reversal potentials to more negative values, the error being even throughout the range of $[K^+]_o$. It cannot, therefore, explain our observations. It is unlikely that Na^+ permeation of $I_{K(N)}$ channels is significant, because substituting most of the extracellular Na^+ with TEA^+ did not change the reversal potential in the presence of physiological $[K^+]_o$. Long prepulses at positive potentials have been shown to cause a positive shift in the reversal potential of a delayed rectifier current, most probably through accumulation of K^+ around the channel mouth (Smirnov & Aaronson, 1994). Such an effect would be greatest at low $[K^+]_o$, producing progressively less interference as the $[K^+]_o$ is raised. Thus K^+ accumulation could produce deviation of the reversal potential from Nernstian behaviour similar to that observed. Nevertheless, since the measured values in Fig. 3*B* closely fit the predictions of eqn (2), the simplest explanation is that the current observed during negative voltage ramps from 0 mV reflects a combination of $I_{K(N)}$ and a leakage current. The K^+ selectivity of $I_{K(N)}$ was confirmed by the finding that the

non-inactivating, outwardly rectifying current was abolished by replacing the intracellular K^+ with Cs^+.

Properties of $I_{K(N)}$

Like other voltage-gated K^+ currents, $I_{K(N)}$ showed a sigmoidal dependence on voltage, displaying rectification that was outward at negative potentials and inward at positive potentials. Several properties of $I_{K(N)}$ distinguish it, however, from other voltage-gated K^+ currents that coexist in the same cells, in particular $I_{K(A)}$ and $I_{K(V)}$. For example, $I_{K(N)}$ has a lower activation threshold. During depolarizing steps or ramps from negative potentials in the presence of high $[K^+]_o$, current could first be resolved at −65 mV. It is likely that the threshold is more negative than that, because after fully activating $I_{K(N)}$ at 0 mV, subsequent steps or ramps to negative potentials did not produce maximal deactivation until close to −80 mV. The finding in physiological $[K^+]_o$ that long prepulses to between −70 mV and −60 mV caused the recruitment of extra current during a subsequent test pulse, is also consistent with a more negative activation threshold. Thus the threshold lies between −80 and −65 mV. In addition, $I_{K(N)}$ attains maximal open probability by around −40 mV, where $I_{K(A)}$ and $I_{K(V)}$ are minimal. Activation of $I_{K(N)}$ occurs without a delay but is very slow. At −60 mV, activation followed a simple mono-exponential time course with a time constant of 1·6 s. By comparison, activation of $I_{K(A)}$ and $I_{K(V)}$ is complete within 100 ms of a step to −40 mV or above (Clapp & Gurney, 1991; Evans *et al.* 1994). Once activated at 0 mV, $I_{K(N)}$ failed to inactivate while the smooth muscle cell remained depolarized, even after periods longer than 10 min. This allowed it to be separated from $I_{K(A)}$ and $I_{K(V)}$, since it remained active after the latter currents had maximally inactivated. Pharmacological differences also enabled $I_{K(N)}$ to be distinguished from $I_{K(A)}$ and $I_{K(V)}$. At 10 μM, quinine caused > 50% inhibition of the latter currents while having either no effect or causing augmentation of $I_{K(N)}$. All three currents were substantially suppressed by 10 mM 4-AP, but at lower concentrations the drug may show marginal selectivity for $I_{K(V)}$ and $I_{K(A)}$. The lack of sensitivity of $I_{K(N)}$ to glibenclamide and TEA meant that it could, in addition, be clearly separated from $I_{K(ATP)}$ and $I_{K(Ca)}$, also present in rabbit pulmonary artery smooth muscle cells.

Comparison with other non-inactivating voltage-gated K^+ currents

$I_{K(N)}$ is clearly distinguishable from non-inactivating, voltage-gated K^+ currents that have been characterized in other tissues. The slowly activating and non-inactivating delayed rectifier (min-K, or $I_{K(VS)}$) identified in cardiac myocytes (Sanguinetti & Jurkiewicz, 1990; Varnum, Busch, Bond, Maylie & Adelman, 1993) is different in three important ways: (1) its threshold for activation lies positive to −50 mV; (2) there is little activation at −40 mV, with only 50% achieved by −4 mV; and (3) fits to the time course of activation require three exponential components, reflecting an initial delay and sigmoidal kinetics. Similar distinctions can be drawn between $I_{K(N)}$ and the $aK_V5.1$ channel cloned recently from *Aplysia* (Zhao, Rassendren, Kaang, Furukawa, Kubo & Kandel, 1994).

The kinetic properties of $I_{K(N)}$ do, however, bear striking similarities to those of the M-current ($I_{K(M)}$), which was first identified in sympathetic neurones (Brown & Adams, 1980) and has since been reported in smooth muscle (Sims, Singer & Walsh, 1985). Like $I_{K(N)}$, $I_{K(M)}$ has a threshold for gating close to −65 mV, activates slowly and is non-inactivating (Brown & Adams, 1980; Brown, 1988). There are, however, important differences. Although $I_{K(M)}$ activation follows a simple exponential time course, the time constant, usually < 200 ms at −60 mV (Brown & Adams, 1980; Brown, 1988), is faster than that found for $I_{K(N)}$ at the same potential. Deactivation of $I_{K(M)}$ also follows an exponential time course, but at a common potential, deactivation follows the same kinetics as $I_{K(M)}$ activation (e.g. Brown & Adams, 1980). Thus $I_{K(M)}$ displays symmetric kinetics of activation and deactivation. This property clearly distinguishes $I_{K(M)}$ from $I_{K(N)}$, which displayed asymmetric activation and deactivation kinetics, activation being more than an order of magnitude slower than deactivation. A more important distinction, perhaps, is that $I_{K(N)}$ was not inhibited by the muscarinic agonist carbachol (authors' unpublished observation), even though muscarinic activation suppresses the smooth muscle (Sims *et al.* 1985) and neuronal (Marrion, Smart & Brown, 1987; Brown, 1988) $I_{K(M)}$ under similar conditions. Furthermore, $I_{K(M)}$ is blocked by millimolar concentrations of Ba^{2+} (Brown, 1988), which had no effect on $I_{K(N)}$. Similar distinctions can be made between $I_{K(N)}$ and currents described in a number of other cell types that resemble $I_{K(M)}$ (e.g. Beech & Barnes, 1989; Hughes, Takahira & Segawa, 1995). There is a closer similarity between $I_{K(N)}$ and $I_{K(M)}$ recorded from fetal rat superior cervical ganglia (Marrion *et al.* 1987) and C cells of bullfrog sympathetic ganglia (Jones, 1987), where the current is not coupled to muscarinic receptors. Nevertheless, $I_{K(M)}$ in all cells studied to date has exhibited symmetric activation and deactivation kinetics, clearly distinguishing it from $I_{K(N)}$.

In summary, we have identified a novel K^+ conductance in rabbit pulmonary artery myocytes, which can be identified by its distinct pharmacology and kinetics. The K^+ channels that underlie $I_{K(N)}$ are likely to be members of the voltage-gated K^+ channel superfamily, and may be of major importance to the physiological and pathophysiological control of pulmonary arterial tone.

BEECH, D. J. & BARNES, S. (1989). Characterization of a voltage-gated K^+ channel that accelerates the rod response to dim light. *Neuron* **3**, 573–581.

BEECH, D. J. & BOLTON, T. B. (1989). Two components of potassium current activated by depolarization of single smooth muscle cells from the rabbit portal vein. *Journal of Physiology* **418**, 293–309.

BENHAM, C. D., BOLTON, T. B., LANG, R. J. & TAKEWAKI, T. (1986). Calcium-activated potassium channels in single smooth muscle cells of rabbit jejunum and guinea-pig mesenteric artery. *Journal of Physiology* **371**, 45–67.

BRAYDEN, J. E. & NELSON, M. T. (1992). Regulation of arterial tone by activation of calcium-dependent potassium channels. *Science* **256**, 532–535.

BROWN, D. A. (1988). M-currents: an update. *Trends in Neuroscience* **11**, 294–299.

BROWN, D. A. & ADAMS, P. R. (1980). Muscarinic suppression of a novel voltage-sensitive K^+ current in a vertebrate neurone. *Nature* **283**, 673–676.

CALLAHAN, M. J. & KORN, S. J. (1994). Permeation of Na through a delayed rectifier K channel in chick dorsal root ganglia neurones. *Journal of General Physiology* **104**, 747–771.

CASTEELS, R., KITAMURA, K., KURIYAMA, H. & SUZUKI, H. (1977*a*). The membrane properties of the smooth muscle cells of the rabbit main pulmonary artery. *Journal of Physiology* **271**, 41–61.

CASTEELS, R., KITAMURA, K., KURIYAMA, H. & SUZUKI, H. (1977*b*). Excitation–contraction coupling in the smooth muscle cells of the rabbit main pulmonary artery. *Journal of Physiology* **271**, 63–79.

CLAPP, L. H. & GURNEY, A. M. (1991). Outward currents in rabbit pulmonary artery cells dissociated with a new technique. *Experimental Physiology* **76**, 677–693.

CLAPP, L. H. & GURNEY, A. M. (1992). ATP-sensitive potassium channels regulate the resting potential of pulmonary arterial smooth muscle cells. *American Journal of Physiology* **262**, H916–920.

EDWARDS, F. R., HIRST, G. D. S. & SILVERBERG, G. D. (1988). Inward rectification in rat cerebral arterioles: involvement of potassium ions in autoregulation. *Journal of Physiology* **404**, 455–466.

EVANS, A. M., CLAPP, L. H. & GURNEY, A. M. (1994). Augmentation by intracellular ATP of the delayed rectifier current independently of the glibenclamide-sensitive K-current in rabbit arterial myocytes. *British Journal of Pharmacology* **111**, 972–974.

HAEUSLER, G. & THORENS, S. (1980). Effects of tetraethylammonium chloride on contractile, membrane and cable properties of rabbit artery muscle. *Journal of Physiology* **303**, 203–224.

HUGHES, B. A., TAKAHIRA, M. & SEGAWA, Y. (1995). An outwardly rectifying K^+ current active near resting potential in human retinal pigment epithelial cells. *American Journal of Physiology* **269**, C179–187.

JONES, S. W. (1987). A muscarine-resistant M-current in C cells of bullfrog sympathetic ganglia. *Neuroscience Letters* **74**, 309–314.

LANGTON, P. D. (1993). Calcium channel currents recorded from isolated myocytes of rat basilar artery are stretch sensitive. *Journal of Physiology* **471**, 1–11.

LEE, S. H. & EARM, Y. E. (1994). Caffeine induces periodic oscillations of Ca^{2+}-activated K^+ current in pulmonary arterial smooth muscle cells. *Pflügers Archiv* **426**, 189–198.

MARRION, N. V., SMART, T. G. & BROWN, D. A. (1987). Membrane currents in adult rat superior cervical ganglia in dissociated tissue culture. *Neuroscience Letters* **77**, 55–60.

NELSON, M. T., CHENG, H., RUBART, M., SANTANA, L. F., BONEV, A. D., KNOT, H. J. & LEDERER, W. J. (1995). Relaxation of arterial smooth muscle by calcium sparks. *Science* **270**, 633–637.

NELSON, M. T. & QUAYLE, J. M. (1995). Physiological roles and properties of potassium channels in arterial smooth muscle. *American Journal of Physiology* **268**, C799–822.

OKABE, K., KITAMURA, K. & KURIYAMA, H. (1987). Features of a 4-aminopyridine sensitive outward current observed in single smooth muscle cells from the rabbit pulmonary artery. *Pflügers Archiv* **409**, 561–568.

POST, J. M., GELBAND, C. H. & HUME, J. R. (1995). $[Ca^{2+}]_i$ inhibition of K^+ channels in canine pulmonary artery. Novel mechanism for hypoxia-induced membrane depolarization. *Circulation Research* **77**, 131–139.

POST, J. M., HUME, J. R., ARCHER, S. L. & WEIR, E. K. (1992). Direct role for potassium channel inhibition in hypoxic pulmonary vasoconstriction. *American Journal of Physiology* **262**, C882–890.

QUAYLE, J. M. & STANDEN, N. B. (1994). K_{ATP} channels in vascular muscle. *Cardiovascular Research* **28**, 797–804.

ROBERTSON, B. E., CORRY, P. R., NYE, P. C. G. & KOZLOWSKI, R. Z. (1992). Ca^{2+} and Mg-ATP activated potassium channels from rat pulmonary artery. *Pflügers Archiv* **421**, 97–99.

SAFRONOV, B. V. & VOGEL, W. (1995). Modulation of delayed rectifier K^+ channel activity by external K^+ ions in *Xenopus* axon. *Pflügers Archiv* **430**, 879–886.

SANGUINETTI, M. C. & JURKIEWICZ, N. K. (1990). Two components of cardiac delayed rectifier K^+ current: Differential sensitivity to block by class III antiarrhythmic agents. *Journal of General Physiology* **96**, 195–215.

SIMS, S. M., SINGER, J. J & WALSH, J. V. (1985). Cholinergic agonists suppress a potassium current in freshly dissociated smooth muscle cells of the toad. *Journal of Physiology* **367**, 503–529.

SMIRNOV, S. V. & AARONSON, P. I. (1994). Alteration of the transmembrane K^+ gradient during development of delayed rectifier in isolated rat pulmonary arterial cells. *Journal of General Physiology* **104**, 241–264.

SMIRNOV, S. V., ROBERTSON, T. P., WARD, J. P. & AARONSON, P. I. (1994). Chronic hypoxia is associated with reduced delayed rectifier K^+ current in rat pulmonary artery muscle cells. *American Journal of Physiology* **266**, H365–370.

SUTTER, K. J., TURNER, J. L., ALBARWANI, S., CLAPP, L. H. & KOZLOWSKI, R. Z. (1995). Ca^{2+}-activated Cl^- and K^+ channels and their modulation by endothelin-1 in rat pulmonary arterial smooth muscle cells. *Experimental Physiology* **80**, 815–824.

SUZUKI, H. & TWAROG, B. M. (1982). Membrane properties of smooth muscle cells in pulmonary arteries of the rat. *American Journal of Physiology* **242**, H900–906.

SWENSON, R. P. & ARMSTRONG, C. M. (1981). K^+ channels close more slowly in the presence of external K^+ and Rb^+. *Nature* **291**, 427–429.

TRIESCHMANN, U. & ISENBERG, G. (1989). Ca^{2+}-activated K^+ channels contribute to the resting potential of vascular myocytes. Ca^{2+} sensitivity is increased by intracellular Mg^{2+} ions. *Pflügers Archiv* **414**, suppl. 1, S183–184.

TURNER, J. L., CHANG, A. S., BROWN, A. M. & KOZLOWSKI, R. Z. (1996). Molecular characterization of K^+ channels in rat pulmonary arterial smooth muscle and their relationship to oxygen sensation. *Journal of Physiology* **491.P**, 21*P*.

VARNUM, M. D., BUSCH, A. E., BOND, C. T., MAYLIE, J. & ADELMA, J. P. (1993). The min K channel underlies the cardiac potassium current $I_{(KS)}$ and mediates species specific responses to protein kinase C. *Proceedings of the National Academy of Sciences of the USA* **90**, 11528–11532.

YUAN, X.-J. (1995). Voltage-gated K^+ currents regulate resting membrane potential and $[Ca^{2+}]$ in pulmonary arterial myocytes. *Circulation Research* **77**, 370–378.

ZHAO, B., RASSENDREN, F., KAANG, B.-K., FURUKAWA, Y., KUBO, T. & KANDEL, E. R. (1994). A new class of non-inactivating K^+ channels from aplysia capable of contributing to the resting potential and firing patterns of neurons. *Neuron* **13**, 1205–1213.

Acknowledgements

Financial support for this study was provided by the British Heart Foundation and the Royal Society.

Author's present address

A. M. Evans: Department of Pharmacology, University of Oxford, Mansfield Road, Oxford OX1 3QT, UK.

Author's email address

A. M. Gurney: a.m.gurney@strath.ac.uk

Received 19 February 1996; accepted 8 July 1996.